

WICA: nonlinear weighted ICA

Andrzej Bedychaj¹ and Przemysław Spurek and Aleksandra Nowak and Jacek Tabor

Abstract. Independent Component Analysis (ICA) aims to find a coordinate system in which the components of the data are independent. In this paper we construct a new nonlinear ICA model, called WICA, which obtains better and more stable results than other algorithms. A crucial tool is given by a new efficient method of verifying nonlinear dependence with the use of computation of correlation coefficients for normally weighted data. Our code for WICA is available on Github².

1 Introduction

Linear Independent Components Analysis (ICA) is an important data analysis technique, which aims to identify a *linear* function such that the components of the dataset obtained after the transformation are independent. Commonly, the independence is approximated using some measure of nongaussianity, e.g. kurtosis (Hyvärinen 1999, Bell & Sejnowski 1995), skewness (Spurek et al. 2017). Clearly, the obvious limitation of ICA is the restriction to linear transformations, as the real world data usually contains complex, nonlinear dependencies, see for instance (Larson 1998), (Ziehe et al. 2000). Designing an efficient and easily implementable nonlinear analogue of ICA is a much more complex problem than its linear counterpart. A fundamental problem is that the solution of nonlinear ICA is in principle non-identifiable, as without any constraints on the space of the mixing functions, there exists an infinite number of valid solutions (Hyvärinen & Pajunen 1999). However, the key challenge in developing nonlinear variant of ICA lies in devising an efficient measure of independence.

One of the most common nonlinear method is MISEP (Almeida 2003) which, similar to the popular INFOMAX algorithm (Bell & Sejnowski 1995), uses the mutual information criterion. In consequence, the procedure involves the calculation of the Jacobian of the modeled nonlinear transformation, which often causes a computational overhead when both the input and output dimensions are large. Another approach is applied in NICE (Dinh et al. 2014). Authors propose a fully invertible neural network architecture where the Jacobian is trivially obtained. The independent components are then estimated using the maximum likelihood criterion. The drawback of both MISEP and NICE is that they require choosing the prior distribution family of the unknown independent components. An alternative approach is given by ANICA (Adversarial Non-linear ICA) (Brakel & Bengio 2017), where the independence measure is directly learned in each task with the use of GAN-like adversarial approach. They show that GAN based independency measure combined with an autoencoder architecture can be used to solve nonlinear blind source separation problems. Unfortunately, the use of adversarial training in

ANICA comes at the cost of added instability, which was also noted by the authors.

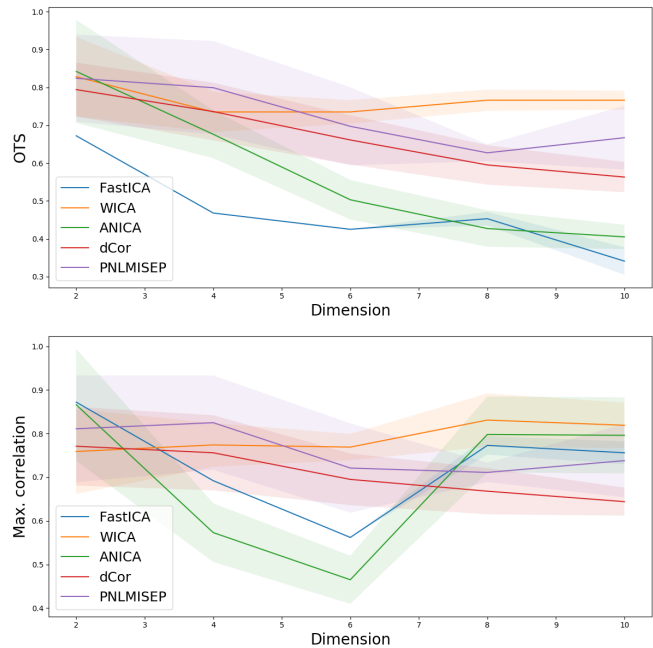


Figure 1. Comparison between standard ICA methods (PNLMISEP, dCor, ANICA, FastICA) and our approach (WICA) on classical source separation problem by using max correlation and OTS measures. In the experiment we train five models and present mean and standard deviation. One can observe that WICA not only outperform other methods in both measures for selected task, but also is the most stable across all dimensions took into consideration. Numerical results of the experiment are presented in Table 1.

Our main contribution is *developing an effective independence measure that does not require adversarial training, and matches ANICA performance*. In other words, we found that the adversarial training is not the key contributor to the efficacy of the ANICA.

In this paper we present a competitive approach to non-linear independent components analysis – WICA (nonlinear weighted ICA). Crucial role in our approach is played by the conclusion from (Bedychaj et al. 2019), which proves that to verify nonlinear independence it is sufficient to check the linear independence of the normally weighted dataset, see Fig. 2. Based on this result we introduce *weighted independence index* (wii) which is based on computing weighted covariance and can be applied to the verification of the nonlinear independence, see Section 2. Consequently, the con-

¹ Jagiellonian University, Poland, email: andrzej.bedychaj@gmail.com

² <https://github.com/gmum/wica>

structured WICA algorithm is based on simple operations on matrices, and therefore is ideal for GPU calculation and parallel processing. We construct it by incorporating the introduced cost function in a commonly used in ICA problems auto-encoder framework (Brakel & Bengio 2017, Le et al. 2011), where the role of the decoder is to limit the unmixing function so that the learned by the decoder independent components contain the information needed to reconstruct the inputs, see Section 3.

We verified our algorithm in the case of a source signal separation problem. We present the results of WICA for nonlinear mixes of images and for the decomposition of electroencephalogram signals. It occurs that WICA outperforms other methods of nonlinear ICA, both with respect to unmixing quality and the stability of the results, see Fig. 1.

To fairly evaluate various nonlinear ICA methods in the case of higher dimensional datasets, we introduce a new index called OTS based on Spearman’s rank correlation coefficient. In the definition of OTS, similarly to clustering accuracy (ACC) (Cai et al. 2005, 2010), we use optimal transport to obtain the minimal mismatch cost. This approach has its merit here, since the correspondence between the input coordinates and the reconstructed components in a higher dimensional space is nontrivial.

Another important ingredient of the paper is the introduction of a new, fully invertible nonlinear mixing function. In the case of linear ICA there exists many experiments settings that can be used in order to evaluate and compare different methods. Such standards are unfortunately not present in the case of nonlinear ICA. Therefore it is not clear what kind of nonlinear mixing should be used in the benchmark experiments. In most cases the authors usually use mixing functions, which correspond with the models architecture (Almeida 2003, Brakel & Bengio 2017). In the paper we propose a new nonlinear mixing function based on the flow models (Dinh et al. 2014, Kingma & Dhariwal 2018), which can be used for verification of nonlinear methods.

2 Weighted independence index

Let us consider a random vector \mathbf{X} in \mathbb{R}^d with density f . Then \mathbf{X} has independent components iff f factors as

$$f(x_1, \dots, x_d) = f_1(x_1) \cdot \dots \cdot f_d(x_d),$$

for some densities f_i , where $i \in \{1, 2, \dots, d\}$. This functions are called marginal densities of f . A related, but much weaker notion, is the linear independence. We say that \mathbf{X} has uncorrelated (linearly independent) components, if the covariance of \mathbf{X} is diagonal. Contrary to the independence, correlation (linear independence) has fast and easy to compute estimators. Clearly independence implies linear independence, but the opposite is not valid., see Fig. 2.

Let us mention that there exist other measures which verify the independence. One of the most well-known measures of independence of random vectors is the *distance correlation* (dCor) (Székely et al. 2007), which is applied in (Matteson & Tsay 2017) to solve the linear ICA problem. Unfortunately, to verify the independence of components of the samples, dCor needs $2^d N^4$ comparisons, where d is the dimension of the sample and N is the sample size. Moreover, even a simplified version of dCor which checks only pairwise independence has high complexity and does not obtain very good results (which can be seen in experiments from Section 5). This motivates the research into fast, stable and efficient measures of independence, which are adapted to GPU processing.

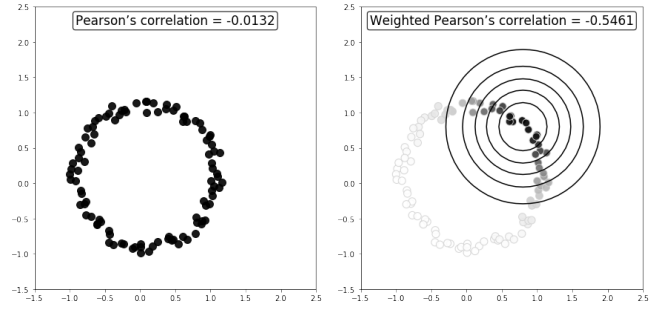


Figure 2. Sample from a random vector which Pearson’s correlation is equal to zero (left), but the components are not independent. Since the components are not independent, one can choose Gaussian weights so that Pearson’s correlation of weighted dataset is not zero (right).

In this section we fill this gap and introduce a method of verifying independence which is based on the covariance of the weighted data. The covariance scales well with respect to the sample size and data dimension, therefore the proposed covariance-based index inherits similar properties.

To proceed further, let us introduce weighted random vectors.

Definition 2.1. Let $w : \mathbb{R}^d \rightarrow \mathbb{R}_+$ be a bounded weighting function. By \mathbf{X}_w we denote a weighted random vector with a density³

$$f_w(x) = \frac{w(x)f(x)}{\int w(z)f(z)dz}.$$

Observation 2.1. Let \mathbf{X} be a random vector which has independent components, and let w be an arbitrary weighting function. Then \mathbf{X}_w has independent components as well.

One of the main results of (Bedychaj et al. 2019) is that the strong version of the inverse of the above theorem holds. Given $m \in \mathbb{R}^d$, we consider the weighting of \mathbf{X} by the standard normal gaussian with center at m ($N(m, \mathbb{I})$):

$$\mathbf{X}_{[m]} = \mathbf{X}_{N(m, \mathbb{I})}.$$

We quote the following result which follows directly from the proof of Theorem 2 from (Bedychaj et al. 2019):

Theorem 2.1. Let \mathbf{X} be a random vector, let $p \in \mathbb{R}^d$ and $r > 0$ be arbitrary.

If $\mathbf{X}_{[q]}$ has linearly independent components for every $q \in B(p, r)$, where $B(p, r)$ is a ball with center in p and radius r , then \mathbf{X} has independent components.

Given sample $X = (x_i) \subset \mathbb{R}^d$, vector $p \in \mathbb{R}^d$, and weights $w_i = N(p, \mathbb{I})(x_i)$, we define the weighted sample as:

$$X_{[p]} = (x_i, w_i).$$

Then the mean and covariance for the weighted sample $X_{[p]} = (x_i, w_i)$ is given by:

$$\text{mean}X_w = \frac{1}{\sum_i w_i} \sum_i w_i x_i$$

and

$$\text{cov}X_w = \frac{1}{\sum_i w_i} \sum_i w_i (x_i - \text{mean}X_w)(x_i - \text{mean}X_w)^T.$$

³ This is just the normalization of $w(x)f(x)$.

The informal conclusion from the above theorem can be stated as follows: if $\text{cov}X_{[p]}$ is (approximately) diagonal for a sufficiently large set of p , then the sample X was generated from a distribution with independent components.

Let us now define an index which will measure the distance from being independent. We define the *weighted independence index* - $\text{wii}(X, p)$ - as

$$\text{wii}(X, p) = \frac{2}{d(d-1)} \sum_{i < j} c_{ij},$$

where d is the dimension of X and

$$c_{ij} = \frac{2z_{ij}^2}{z_{ii}^2 + z_{jj}^2},$$

for $Z = [z_{ij}] = \text{cov}X_{[p]}$.

Observation 2.2. Let us first observe that c_{ij} is a close measure to the correlation ρ_{ij} , namely:

$$c_{ij} \leq \rho_{ij}^2,$$

where the equality holds iff the i -th and j -th components in $X_{[p]}$ have equal standard deviations.

Proof. Obviously

$$\rho_{ij}^2 = \frac{z_{ij}^2}{z_{ii} \cdot z_{jj}}.$$

Since $ab \leq \frac{1}{2}(a^2 + b^2)$ (where the equality holds iff $a = b$), we obtain the assertion of the observation. \square

Consequently, $\text{wii}(X, p) = 1$ iff all components of $X_{[p]}$ are linearly dependent and have equal standard deviations. Thus, the minimization of wii simultaneously aims at maximizing the independence and increasing the difference between the standard deviations.

We extend the index for a sequence of points $\{p_1, \dots, p_n\}$, as the mean of the indexes for each p_i :

$$\text{wii}(X; \{p_1, \dots, p_n\}) = \frac{1}{n} \sum_{i=1}^n \text{wii}(X, p_i).$$

3 Description of the WICA algorithm

To implement the weighted independence index in practice, we need to find the optimal choice of weighting centers (p_i). First, we assume that the dataset in question is normalized componentwise (in particular, variance of each coordinate is one). We argue that the right choice of (p_i) should satisfy the following two conditions:

- selected weights do not concentrate on a small percentage of the data,
- for different centers selected from the dataset, weights diversify the data points.

At first glance, it would seem that the natural choice for points (p_i) is to sample them from the standard normal distribution. However, the conducted by us preliminary experiments (see Fig. 3) demonstrate that sampling from $N(0, \mathbb{I}/d)$ would be a better choice.

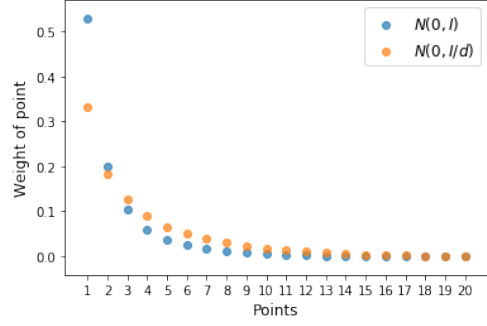


Figure 3. In the experiment, we sampled twenty points from $N(0, \mathbb{I})$ (x-axis). Then, we calculate weights of the points respectively to $N(0, \mathbb{I})$ and $N(0, \mathbb{I}/d)$. We present values of those weights (sorted decreasingly) in the case when the center is chosen according to $N(0, \mathbb{I})$ vs. $N(0, \mathbb{I}/d)$. One can see that weights derived from $N(0, \mathbb{I}/d)$ actually balance more data points, in contrary to $N(0, \mathbb{I})$ which focus on smaller amount of data.

Theoretical analysis. Let us now discuss the theoretical foundations behind the results from Fig. 3. Consider the case when the data come from the standard normal distribution. For given weights w and density f we define measure $P(w, f)$ as:

$$P(w, f) = \frac{(\int w(x)f(x)dx)^2}{\int w^2(x)f(x)dx}. \quad (1)$$

Observe that if w is constant on a subset U of some space S (for which functions w and f are well-defined) and zero otherwise, then the above reduces to $\mu(U)$, where μ is counting measure. Intuitively, $P(w, f)$ *measures percentage of the population which has nontrivial weights*.

Let us consider the case when μ is given by the standard normal density

$$w(x) = N(p, \mathbb{I})(x)$$

and our dataset is normalized as stated above. Then, directly from (1), one obtains:

$$P(w, f) = \frac{(\int N(p, \mathbb{I})(x)N(0, \mathbb{I})(x)dx)^2}{\int N(p, \mathbb{I})^2(x)N(0, \mathbb{I})(x)dx}$$

Applying the formula for the product of two normal densities:

$$N(m_1, \Sigma_1)(x) \cdot N(m_2, \Sigma_2)(x) = c_c N(m_c, \Sigma_c)(x),$$

where

$$c_c = N(m_1 - m_2, \Sigma_1 + \Sigma_2)(0),$$

$$\Sigma_c = (\Sigma_1^{-1} + \Sigma_2^{-1})^{-1},$$

and

$$m_c = \Sigma_c(\Sigma_1^{-1}m_1 + \Sigma_2^{-1}m_2),$$

we get:

$$\int N(p, \mathbb{I})(x)N(0, \mathbb{I})(x)dx = N(p, 2\mathbb{I})(0),$$

for the numerator, and

$$\int N(p, \mathbb{I})^2(x)N(0, \mathbb{I})(x)dx = N(0, 2\mathbb{I})(0)N(p, \frac{3}{2}\mathbb{I})(0).$$

for the denominator. The equation for the denominator follows from the simple fact that:

$$N(p, \mathbb{I})^2(x) = N(0, 2\mathbb{I})(0) \cdot N(p, \frac{1}{2}\mathbb{I})(x),$$

Summarizing, we obtain that

$$\begin{aligned} P(N(p, \mathbb{I}), N(0, \mathbb{I})) &= \frac{N(p, 2\mathbb{I})^2(0)}{N(0, 2\mathbb{I})(0)N(p, \frac{3}{2}\mathbb{I})(0)} \\ &= (\frac{3}{4})^{D/2} \exp(-\frac{1}{6}\|p\|^2). \end{aligned} \quad (2)$$

Normalizing (2) by its maximum obtained at 0, we get

$$\exp(-\frac{1}{6}\|p\|^2).$$

Clearly if p would be chosen from the standard normal distribution, the value of $\|p\|^2$ for large dimensions equals approximately d , and consequently the weights for the randomly chosen points will become concentrated at single point (see Fig 3). To obtain the quotient approximately constant, we should choose p so that its norm is approximately one. Hence, it leads to the choice of p from the distribution $N(0, \frac{1}{d}\mathbb{I})$.

One can observe, that if $\mathbf{X} \sim N(0, \mathbb{I})$, then we can sample from $N(0, \mathbb{I}/d)$ by taking the mean of d randomly chosen vectors from \mathbf{X} . This leads to the following definition:

Definition 3.1. For the dataset $X \subset \mathbb{R}^d$, we define

$$\text{wii}(X) = \mathbb{E}\{\text{wii}(Y, p) : p \text{ a mean of random } d \text{ elements of } Y\},$$

where Y is a componentwise normalization of X and \mathbb{E} stands for expected value.

Let us summarize why centering the weights at the mean of d elements from the dataset has good properties:

- if the data is restricted to some subspace S of the space, then mean also belongs to S ;
- if the data comes from normal distribution $N(m, \Sigma)$, then mean of d elements comes from $N(m, \Sigma/d)$,
- if the data has heavy tails (i.e. comes from Cauchy distribution), then the distribution of mean for d elements set can be close to the original dataset mean.

The realisation of this idea in practice is provided by our algorithm – WICA – a nonlinear ICA model based on the wii index. Following the ANICA (Brakel & Bengio 2017), we used an Auto-Encoder (AE) architecture.

Auto-Encoder model. Let $X \subset \mathbb{R}^d$ denote the input data. An Auto-Encoder is a model consisting of an encoder function $\mathcal{E} : \mathbb{R}^d \rightarrow \mathcal{Z}$ and a complementary decoder function $\mathcal{D} : \mathcal{Z} \rightarrow \mathbb{R}^d$, aiming to enforce coding of the input variables that minimizes the reconstruction error:

$$\text{rec_error}(X; \mathcal{E}, \mathcal{D}) = \sum_{i=1}^d \|x_i - \mathcal{D}(\mathcal{E}x_i)\|^2.$$

WICA cost function. In this paragraph we describe the actual cost function used in the WICA model.

To obtain independence in the latent space, we add to the standard Auto-Encoder cost function the weighted independence index wii computed in the latent. Thus our final cost function is given by

$$\text{cost}(X; \mathcal{E}, \mathcal{D}) = \text{rec_error}(X; \mathcal{E}, \mathcal{D}) + \beta \text{wii}(\mathcal{E}X). \quad (3)$$

where β is a hyperparameter which aims to weight the role of reconstruction with that of independence (analogous to β -VAE (Higgins et al. 2017)). The training procedure follows the steps:

Algorithm 1 WICA

1. Take mini-batch X' from the dataset X .
2. Normalize componentwise $\mathcal{E}X'$, to obtain Y
3. Compute p_1, \dots, p_d , where p_i is the mean of randomly chosen d elements from Y ,
4. Minimize:

$$\text{rec_error}(X'; \mathcal{E}, \mathcal{D}) + \beta \text{wii}(Y; p_1, \dots, p_d).$$

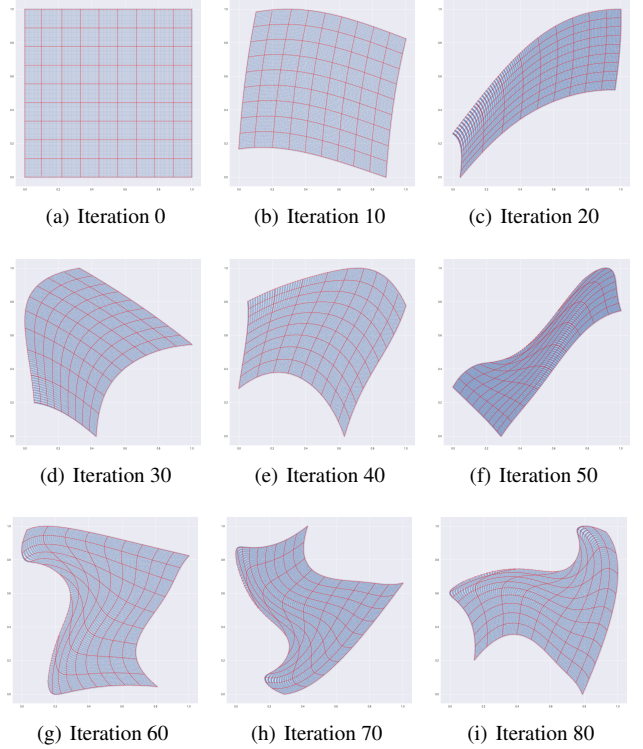


Figure 4. Results of the proposed mixing over synthetic lattice data. One may observe that after multiple iterations of the proposed mixing, results become highly nonlinear.

4 Setting up the experiments

Nonlinear mixing. We start this section with a discussion of possible definitions of the nonlinear mixing function used for benchmarking the ICA methods. In the beginning we shortly explain some approaches used in the linear ICA, and then move forward to propose a mixing which benefits from properties desired in the comparison of the results obtained by nonlinear ICA algorithms.

In the case of linear ICA the experiments are usually conveyed on an artificial dataset, which is obtained by mixing two or more of independent source signals. This allows for the comparison of the results returned by the analyzed methods with the original independent components. In real-world applications such a procedure is of course infeasible, but in experimental setting it provides a good basis for benchmarking different models. In classical ICA setup, creating an artificial mixing function is equivalent to selecting a random invertible matrix A , such that $X = A \cdot S$, where S are the true sources and X are the observations, which are then passed to the evaluated

Measure	Dim	Mixes	WICA	FastICA	ANICA	dCor	PNLMISEP
OTS	2	50	0.828 ± 0.105	0.672 ± 0.001	0.842 ± 0.136	0.794 ± 0.071	0.824 ± 0.115
	4	50	0.735 ± 0.053	0.468 ± 0.001	0.676 ± 0.063	0.736 ± 0.076	0.799 ± 0.123
	6	50	0.735 ± 0.031	0.425 ± 0.001	0.503 ± 0.052	0.661 ± 0.065	0.697 ± 0.103
	8	50	0.766 ± 0.028	0.453 ± 0.018	0.427 ± 0.048	0.595 ± 0.052	0.627 ± 0.022
	10	50	0.766 ± 0.025	0.341 ± 0.036	0.405 ± 0.032	0.563 ± 0.040	0.667 ± 0.084
	2	10	0.798 ± 0.048	0.652 ± 0.001	0.938 ± 0.088	0.899 ± 0.076	0.948 ± 0.041
	4	10	0.890 ± 0.065	0.582 ± 0.001	0.784 ± 0.062	0.554 ± 0.264	0.652 ± 0.360
	6	10	0.807 ± 0.043	0.419 ± 0.001	0.571 ± 0.056	0.666 ± 0.064	0.779 ± 0.046
	8	10	0.784 ± 0.025	0.457 ± 0.058	0.431 ± 0.054	0.594 ± 0.051	0.769 ± 0.097
	10	10	0.742 ± 0.030	0.405 ± 0.077	0.405 ± 0.032	0.556 ± 0.041	0.758 ± 0.103
max correlation	2	50	0.759 ± 0.097	0.872 ± 0.001	0.866 ± 0.128	0.771 ± 0.090	0.811 ± 0.122
	4	50	0.774 ± 0.050	0.692 ± 0.001	0.573 ± 0.067	0.756 ± 0.086	0.825 ± 0.108
	6	50	0.769 ± 0.030	0.562 ± 0.001	0.465 ± 0.055	0.695 ± 0.059	0.721 ± 0.102
	8	50	0.831 ± 0.061	0.773 ± 0.021	0.798 ± 0.087	0.668 ± 0.053	0.711 ± 0.022
	10	50	0.819 ± 0.052	0.756 ± 0.026	0.796 ± 0.087	0.644 ± 0.032	0.738 ± 0.084
	2	10	0.771 ± 0.013	0.965 ± 0.001	0.631 ± 0.112	0.901 ± 0.058	0.942 ± 0.045
	4	10	0.910 ± 0.065	0.710 ± 0.001	0.588 ± 0.063	0.552 ± 0.278	0.645 ± 0.363
	6	10	0.821 ± 0.041	0.578 ± 0.001	0.505 ± 0.062	0.696 ± 0.059	0.808 ± 0.063
	8	10	0.814 ± 0.058	0.759 ± 0.046	0.769 ± 0.065	0.658 ± 0.044	0.812 ± 0.085
	10	10	0.812 ± 0.049	0.770 ± 0.058	0.837 ± 0.042	0.658 ± 0.041	0.820 ± 0.077

Table 1. Comparison between nonlinear ICA methods (PNLMISEP, dCor, ANICA, WICA) and the classical linear ICA approach (FastICA) on images separation problem (with different dimensions) by using max correlation and OTS measures. In the experiment we tuned and trained four models (excluding FastICA, which is a linear model) and present mean and standard deviation in the tabular form.

methods. Such mixing is used by (Bedychaj et al. 2019, Hyvärinen 1999, Spurek et al. 2017).

Unfortunately, there do not exist any mixing standards for the nonlinear ICA problem. A common setup of the comparable environments needed to test the nonlinear models of ICA is to interlace linear mixes of signals with nonlinear functions (Almeida 2003, Brakel & Bengio 2017). During our experiments we found that the proposed methods of nonlinear mixes are ineffective in large dimensions. The aforementioned approaches usually apply only a shallow stack of linear projections followed by a non-linearity. In consequence, the obtained observations are either close to the linear mixing (and therefore not hard enough to be properly challenging for the linear models) or become degenerate (i.e. all points cluster towards zero). Because of these disadvantages we propose our own mixing, inspired by (Kingma & Dhariwal 2018, Dinh et al. 2014) network architecture.

Let S be a sample of vectors with independent components. We apply a random isometry on S , by taking $X = (UV^T)S$, where UV^T comes from the Singular Value Decomposition on a random matrix $A_{ij} \sim N(0, 1)$. Next we split $X \in \mathbb{R}^d$ into half

$$(x_i, x_j) \rightarrow (x_i, x_j + \phi(x_i)),$$

similarly as it was done in (Kingma & Dhariwal 2018). Function ϕ is a randomly initialized neural network with two hidden layers and tanh activations after each of them. This approach can be iterated over multiple times to achieve the desired level of nonlinear mixing.

The proposed mixing procedure scales well in higher dimensions by iterating over the splits in \mathbb{R}^d . Additionally, it is also easily invertible, therefore there is a guarantee that the source components may be retrieved. The effects of applying the proposed mixing to two-dimensional data are presented in Fig. 4.

OTS – measuring the quality of nonlinear ICA results. For the benchmark experiments we want to be able to measure the similarity between the obtained results Z and the original sources S . In the case of linear mixing the common choice is the maximum absolute correlation over all possible permutations of the signals (denoted hereafter as *max_corr* (Brakel & Bengio 2017)). However, this measure is based on the Pearson’s correlation coefficient and therefore is not able to catch any high order dependencies. To address this problem

we introduce a new measure based on the nonlinear Spearman’s rank correlation coefficient and optimal transport.

Let Z denote the signal retrieved by an ICA algorithm and let $r_s(z^j, s^k)$ be the Spearman’s rank correlation coefficient between the j -th component of Z and k -th component of S . We define the Spearman’s distance matrix $M(Z, S)$ as

$$M(Z, S) = [1 - |r_s(z^j, s^k)|]_{j,k=1\dots d},$$

where the zero entries indicate a monotonic relationship between the corresponding features.

This matrix is then used as the transportation cost of the components. Formally, we compute the value of the optimal transport problem formulated in terms of integer linear programming:

$$\text{OTS} = 1 - I_s(Z, S),$$

$$I_s(Z, S) = \min_{\gamma} \frac{1}{D} \sum_{j,k} \gamma_{j,k} M(Z, S)_{j,k}$$

subject to:

$$\sum_k \gamma_{j,k} = A_j \text{ for all } j \in \{1, \dots, d\},$$

$$\sum_j \gamma_{j,k} = A_k \text{ for all } k \in \{1, \dots, d\},$$

$$\gamma_{j,k} \in \{0, 1\} \text{ for all } j, k \in \{1, \dots, d\}$$

where $A_j = A_k = 1$.

In consequence of the last constraint, the obtained transport plan γ defines a one-to-one map from the retrieved signals to the original sources. In addition, the proposed Spearman-based measure (OTS) is sensitive to monotonic nonlinear dependencies and also relatively easy to compute with the use of existing tools for integer programming.

5 Experiments

Image separation One of the most figurative application of ICA is the separation of images. The experiment environment in such a

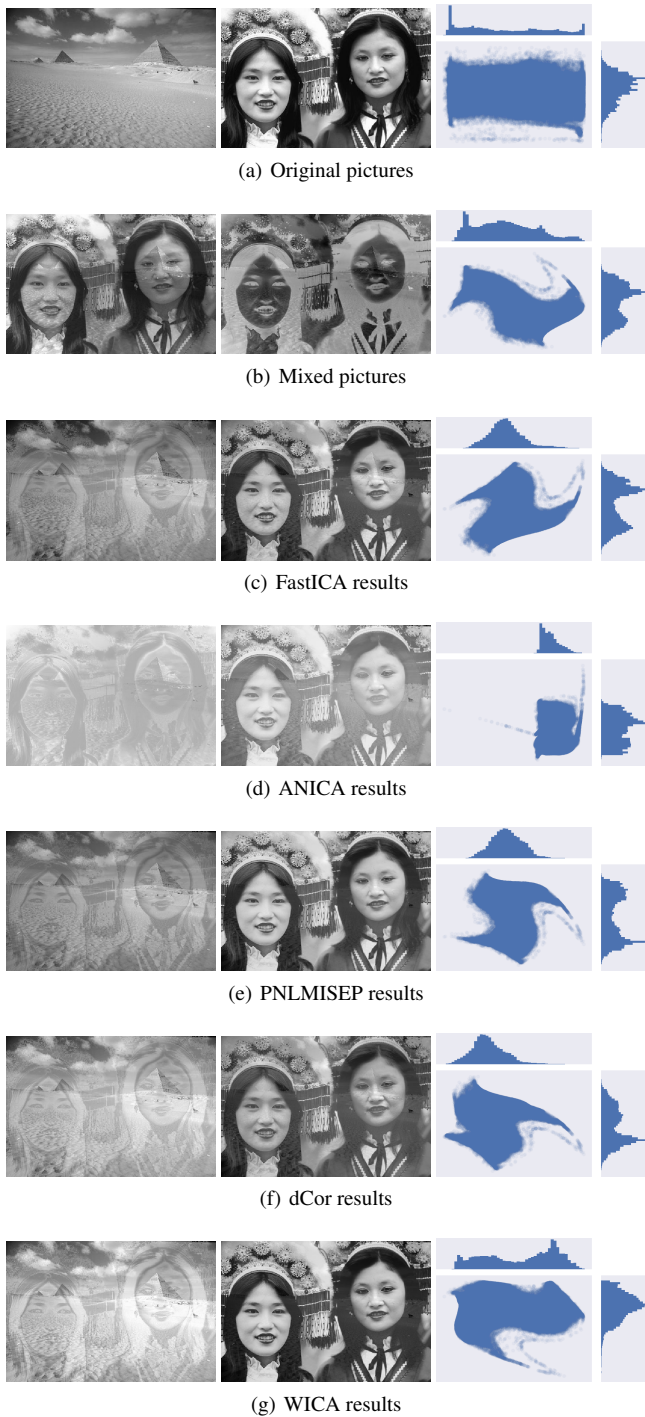


Figure 5. Two dimensional example of unmixing natural images. One can easily spot that WICA has the smallest amount of artifacts persisted after the process of retrieving the signals. All of the scatter plots were normalized and are presented in the same scale. It is valuable to look also on connected marginal histograms, where some of the similarities between original signal and its retrieved counterpart also resembles.

setting is constructed by applying some mixing function to the independent source signal, which are then passed to the tested ICA model.

As a setup for the described blind source separation test, we used

the images from Berkeley Segmentation Dataset⁴ and the mixture defined in Section 4.

For the first demonstration experiment we took random pairs of images, mixed them non-linearly and fed to the analyzed ICA models. The outcome of one of this trials is presented in Fig. 5. We compared the proposed WICA method with dCor (Spurek et al. 2019), PNLMISE (Zheng et al. 2007), ANICA (Bengio et al. 2013) and linear FastICA. One can easily see that WICA produced results closest to the original signals. The marginal densities retrieved by WICA closely resembles those from original images (see Fig. 5).

Next, we verified how WICA compares to other methods in higher dimensions and more complex scenarios. To achieve this goal we performed experiments on $d \in \{2, 4, 6, 8, 10\}$ mixed images. The mixtures are obtained using the function described in Section 4, applied iteratively 10 and 50 times.

We fit each nonlinear algorithm using grid search over the learning rate. For the Auto-Encoder based models we also performed a grid search over the scaling of the independence measure. It is worth to mention that we need to fix batch size to 256, because any bigger value caused instabilities in ANICA results. To be fair in comparisons, we set the same neural net architecture for WICA, ANICA and dCor. Both the encoder and the decoder are composed of 3 hidden layers with 128 neurons each. In case of MISE we used version from (Zheng et al. 2007).

Experiment results measured by max_corr and OTS are shown in Fig. 1. Numeric details for all used methods and measures are presented in Table 1.

The outcomes demonstrate that the WICA method outperformed any of the other nonlinear algorithms in the proposed tasks. WICA handles smaller non-linearities as well as more complex ones. In case of stability of the results WICA losses only to the linear method - FastICA - which unfortunately cannot satisfactorily factorize non-linear data.

This experiment vividly demonstrates that WICA is a strong competitor to other models in well defined environment for nonlinear ICA.

Decomposing EEG data An electroencephalogram (EEG) is a test used to evaluate the electrical activity in the brain. The brain cells communicate via electrical impulses and are active all the time. In the original scalp channel data, each row of the data recording matrix represents the time course of summed voltage differences between source projections to one data channel and one or more reference channels. We followed a common experiment framework proposed in (Onton & Makeig 2006), to detect artifacts in unmixed signals representation which can suggest a blink or an eye movement during the test.

An original EEG mixture taken for this experiment, consisted of 40 scalp electrode signals. Experiment showed that WICA is able to handle multidimensional data highly above tested on other nonlinear models. Moreover, WICA results for this task works well enough to be used as a preliminary step of cleaning the data. Results of WICA decomposition are presented on Fig 6.

6 Conclusion

In this paper we presented a new approach to the nonlinear ICA task. In addition to the investigation of WICA method, which proves to be

⁴ Berkeley Segmentation Dataset

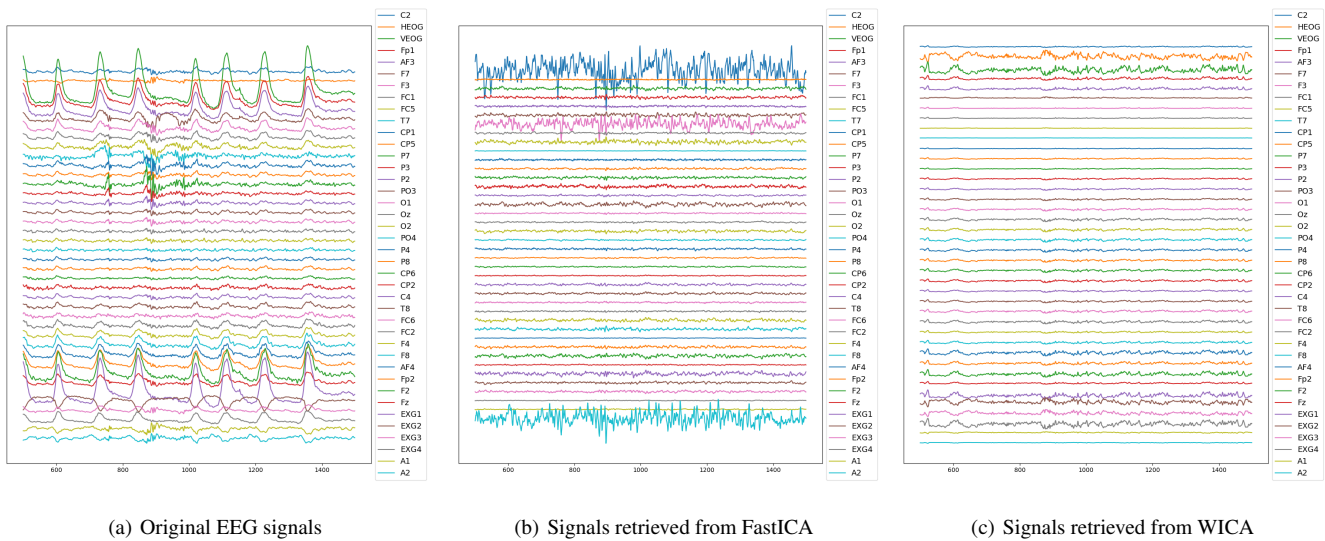


Figure 6. Results of analysis done on EEG signals. After deletion of suspicious signals selected by an expert from decomposition, one can easily spot that the reconstructed signal is more homogeneous, and does not have as much artifacts as the original EEG data. In both methods the same amount of signals was cleared. The results of both methods are satisfying, although it seems that WICA persist scale of the retrieved signals.

matching the results of all other tested nonlinear algorithms, we proposed a new mixing function for validating nonlinear tasks in a structured manner. Our mixing scales to higher dimensions and is easily invertible. Lastly, we defined OTS, a measure that can catch nonlinear dependence and is easy to compute. The OTS measure and the proposed mixing have the potential to become benchmarking tools for all future work in this field.

7 Acknowledgements

The work of P. Spurek was supported by the National Centre of Science (Poland) Grant No. 2019/33/B/ST6/00894. The work of J. Tabor was supported by the National Centre of Science (Poland) Grant No. 2017/25/B/ST6/01271. A. Nowak carried out this work within the research project "Bio-inspired artificial neural networks" (grant no. POIR.04.04.00-00-14DE/18-00) within the Team-Net program of the Foundation for Polish Science co-financed by the European Union under the European Regional Development Fund.

REFERENCES

Almeida, L. B. (2003), 'Misep-linear and nonlinear ica based on mutual information', *Journal of Machine Learning Research* 4(Dec), 1297–1318.

Bedychaj, A., Spurek, P., Struskim, L. & Tabor, J. (2019), 'Independent component analysis based on multiple data-weighting', *arXiv preprint arXiv:1906.00028*.

Bell, A. J. & Sejnowski, T. J. (1995), 'An information-maximization approach to blind separation and blind deconvolution', *Neural computation* 7(6), 1129–1159.

Bengio, Y., Courville, A. & Vincent, P. (2013), 'Representation learning: A review and new perspectives', *IEEE transactions on pattern analysis and machine intelligence* 35(8), 1798–1828.

Brakel, P. & Bengio, Y. (2017), 'Learning independent features with adversarial nets for non-linear ica', *arXiv preprint arXiv:1710.05050*.

Cai, D., He, X. & Han, J. (2005), 'Document clustering using locality preserving indexing', *IEEE Transactions on Knowledge and Data Engineering* 17(12), 1624–1637.

Cai, D., He, X. & Han, J. (2010), 'Locally consistent concept factorization for document clustering', *IEEE Transactions on Knowledge and Data Engineering* 23(6), 902–913.

Dinh, L., Krueger, D. & Bengio, Y. (2014), 'Nice: Non-linear independent components estimation', *arXiv preprint arXiv:1410.8516*.

Higgins, I., Matthey, L., Pal, A., Burgess, C., Glorot, X., Botvinick, M. M., Mohamed, S. & Lerchner, A. (2017), beta-vae: Learning basic visual concepts with a constrained variational framework, in 'ICLR'.

Hyvärinen, A. (1999), 'Fast and robust fixed-point algorithms for independent component analysis', *Neural Networks, IEEE Transactions on* 10(3), 626–634.

Hyvärinen, A. & Pajunen, P. (1999), 'Nonlinear independent component analysis: Existence and uniqueness results', *Neural Networks* 12(3), 429–439.

Kingma, D. P. & Dhariwal, P. (2018), Glow: Generative flow with invertible 1x1 convolutions, in 'Advances in Neural Information Processing Systems', pp. 10215–10224.

Larson, L. E. (1998), 'Radio frequency integrated circuit technology for low-power wireless communications', *IEEE Personal Communications* 5(3), 11–19.

Le, Q. V., Karpenko, A., Ngiam, J. & Ng, A. Y. (2011), Ica with reconstruction cost for efficient overcomplete feature learning, in 'Advances in Neural Information Processing Systems', pp. 1017–1025.

Matteson, D. S. & Tsay, R. S. (2017), 'Independent component analysis via distance covariance', *Journal of the American Statistical Association* pp. 1–16.

Onton, J. & Makeig, S. (2006), Information-based modeling of event-related brain dynamics, in 'Progress in Brain Research', Elsevier, pp. 99–120.

Spurek, P., Nowak, A., Tabor, J., Maziarka, L. & Jastrzebski, S.

- (2019), 'Non-linear ICA based on cramer-wold metric', *CoRR* **abs/1903.00201**.
- Spurek, P., Tabor, J., Rola, P. & Ociepka, M. (2017), 'Ica based on asymmetry', *Pattern Recognition* **67**, 230–244.
- Székely, G. J., Rizzo, M. L., Bakirov, N. K. et al. (2007), 'Measuring and testing dependence by correlation of distances', *The annals of statistics* **35**(6), 2769–2794.
- Zheng, C., Huang, D., Li, K., Irwin, G. & Sun, Z. (2007), 'Misep method for postnonlinear blind source separation', *Neural Computation* **19**(9), 2557–2578.
- Ziehe, A., Muller, K.-R., Nolte, G., Mackert, B.-M. & Curio, G. (2000), 'Artifact reduction in magnetoneurography based on time-delayed second-order correlations', *IEEE Transactions on biomedical Engineering* **47**(1), 75–87.